

UC Merced

UC Merced Previously Published Works

Title

Mechanochemical Association Reaction of Interfacial Molecules Driven by Shear.

Permalink

<https://escholarship.org/uc/item/39t7d1d8>

Journal

Langmuir : the ACS journal of surfaces and colloids, 34(21)

ISSN

0743-7463

Authors

Khajeh, Arash
He, Xin
Yeon, Jejoon
et al.

Publication Date

2018-05-01

DOI

10.1021/acs.langmuir.8b00315

Supplemental Material

<https://escholarship.org/uc/item/39t7d1d8#supplemental>

Peer reviewed

Mechanochemical association reaction of interfacial molecules driven by shearArash Khajeh¹, Xin He², Jejoon Yeon¹, Seong H. Kim^{2*}, and Ashlie Martini^{1*}

¹ Department of Mechanical Engineering, University of California Merced, 5200 N. Lake Road, Merced, CA 95343, USA

² Department of Chemical Engineering and Materials Research Institute, Pennsylvania State University, University Park, Pennsylvania 16802, USA

Abstract: Shear-driven chemical reaction mechanisms are poorly understood because the relevant reactions are often hidden between two solid surfaces moving in relative motion. Here, this phenomenon is explored by characterizing shear-induced polymerization reactions that occur during vapor phase lubrication of α -pinene between sliding hydroxylated and dehydroxylated silica surfaces, complemented by reactive molecular dynamics simulations. The results suggest that oxidative chemisorption of the α -pinene molecules at reactive surface sites, which transfers oxygen atoms from the surface to the adsorbate molecule, is the critical activation step. Such activation takes place more readily on the dehydroxylated surface. During this activation, the most strained part of the α -pinene molecules undergoes a partial distortion from its equilibrium geometry, which appears to be related to the critical activation volume for mechanical activation. Once α -pinene molecules are activated, association reactions occur between the newly attached oxygen and one of the carbon atoms in another molecule, forming ether bonds. These findings have general implications for mechanochemistry since they reveal that shear-driven reactions may occur through reaction pathways very different from their thermally induced counterparts and, specifically, the critical role of molecular distortion in such reactions.

Keywords: mechanochemistry, tribology, shear-induced chemical reactions, ReaxFF MD simulations, vapor phase lubrication

INTRODUCTION

Although not as well-known as thermal, photochemical, and electrochemical reactions, mechanochemical reactions are ubiquitous and play critical roles in natural and engineering systems. Mechanochemistry describes chemical reactions that are induced or facilitated by mechanical force or energy.¹ In biology, examples include the unfolding of protein molecules upon mechanical stretch,²⁻³ shear-induced gene expression and enzyme activation, and mechanically stimulated differentiation of stem cells.⁴⁻⁶ Engineering examples include organic synthesis via ball milling,⁷ rearrangement of macromolecular scaffolds via ultrasonication,⁸ transformation of anti-wear additives forming protective coatings at tribological interfaces,⁹⁻¹² and wear of silica and silicate glass surfaces in humid environments.¹³⁻¹⁴ Among these, chemical reactions at sliding solid interfaces are least understood because of the complexity and dynamic nature of the interfacial conditions which are continuously evolving during the shear.¹⁵⁻¹⁶ The lack of fundamental understanding of chemical reactions induced by shear hampers chemists' ability to design new compounds, such as novel lubricants that can mediate energy waste and material loss at the technically challenging tribological interfaces present in all moving mechanical systems. Herein, we report experimental and computational studies elucidating molecular mechanisms of shear-induced polymerization reactions for a model system: α -pinene molecules adsorbed on sliding interfaces of silicon oxide.

When mechanical or interfacial shear is involved, it is hypothesized that the applied shear stress can facilitate chemical reactions by decreasing the activation energy or changing the reaction path.¹⁷⁻²⁰ These theories also posit the existence of a shear-induced activation volume which is critical to understanding how much a reaction energy barrier is decreased by shear.²¹⁻²² However, due to the complexity of processes during sliding, it is difficult to relate this activation volume to specific physical change.²³ In addition to mechanical shear, the surface chemistry of the sliding solids plays a critical role in determining dominant reaction pathways and kinetics.²⁴⁻²⁶ Intuitively, the molecules chemically anchored to the sliding surface would experience more mechanical shear than the molecules slipping within the interface.²⁷ However, the exact roles of surface chemistry and mechanical shear need to be unraveled for a deeper understanding of mechanochemistry.

Here, the experimental design was inspired by the fact that vapor phase lubrication (VPL) can effectively suppress material loss for most solid surfaces.²⁸ The model system chosen was α -

pinene,²⁹ which has high internal strain due to the presence of the four-membered ring and C=C double bond in the six-membered ring and undergoes mechanochemical polymerization reactions when sheared on a silica surface.³⁰⁻³¹ The hypothesis studied in this work is that chemical reactions between the α -pinene and the silica will facilitate oligomerization during sliding. The experimental results were used to validate reactive molecular dynamics (MD) simulations with a ReaxFF reactive force field, which then revealed mechanistic insights into the shear-induced polymerization of α -pinene on silicon oxide surfaces – especially, the role of chemisorption and shear-induced deformation of molecules which can be generalized to other mechanochemical reactions at sliding interfaces.

METHODS

Experimental Details

Friction tests were conducted with a custom-built reciprocating ball-on-flat tribometer with an environment control capacity.³² The hydroxylated silica substrate was prepared by cleaning a silicon wafer with the RCA-1 solution (5:1:1 mixture of DI water, 30% ammonium hydroxide and 30% hydrogen peroxide at 70 °C) followed by rinsing with DI water and then exposure to UV/ozone. The dehydroxylated silicon substrate was obtained by heating the hydroxylated surface at 450 °C in dry nitrogen for 12 hours, and then cooling to room temperature in dry nitrogen. The counter-surfaces in friction tests were sodium borosilicate glass balls (Pyrex; thermal expansion coefficient = 3.3 ppm/K; diameter = 2.38 mm). The surface roughness was estimated via optical profilometry to be ~4 nm after removal of the ball curvature. The concentration of alpha-pinene was 30~40% p/p_{sat} to ensure the formation of a monolayer on the surface³³. The sliding speed was kept at 4 mm/sec; at this condition, the average flash temperature increase due to friction was estimated to be 4-12 °C only.³² The polymeric products within and aside the slide track were imaged with atomic force microscopy (AFM; Digital instrument, MultiMode). The mechanochemical reaction yield was estimated by normalizing the total volume of products with the sliding area and time. X-ray photoelectron spectroscopy (XPS; PHI, VersaProbe) was used to analyze the chemical composition of the reaction products accumulated in sliding over a $0.2 \times 0.2 \text{ mm}^2$ area.

Computer Simulations

Shear-induced mechanochemical polymerization of α -pinene molecules between two amorphous silica slabs was investigated using ReaxFF-MD simulations (see Figure 1). Two amorphous SiO₂ slabs were created as described in the Supporting Information. A slab-on-slab geometry was chosen for the simulation to represent the elastic flattening of the solid surface in the ball-on-flat contact zone. This also resulted in confinement of reacting molecules within the sliding interface. Note that the roughness of the surfaces in simulations (~ 0.2 nm) was smaller than that of the substrate in experiments (~ 1 nm) due to the length scale limitations of the model. In both cases, the elastic deformation depth under the normal load was larger than the surface roughness. Initially, 31 α -pinene molecules were confined between the amorphous silica slabs, to form approximately a monolayer of α -pinene on each surface. The size of the simulation box was $3.19 \times 3.19 \times 8.00$ nm³. To capture the effect of surface reactivity on the yield, simulations were performed both on non-hydroxylated and hydroxylated surfaces. The non-hydroxylated surface was modeled as silicon oxide produced in the absence of water molecules [see Figure S3]. The hydroxylated surface was created by modeling reactions with water at 500 K [see Figure S4]. The density of defects decreased upon hydroxylation: for example, from ~ 1.2 oxygen radicals per nm² on the non-hydroxylated surface to ~ 0.5 per nm² on the hydroxylated surface [see Figure S5]. Each MD simulation consisted of three main steps: (i) energy minimization and equilibration at 300 K until the energy was stable, (ii) compression by moving the top slab toward the bottom slab in the z-direction at a speed of 5 m/s until the average pressure was approximately equal to the target value (either 1 or 3 GPa), and (iii) sliding the top slab at 10 m/s in the x-direction for 2 ns. Since the flash temperature has been shown to be negligible during sliding in experiments, all simulations were carried out at 300 K by applying the NVT (constant number of atoms, volume and temperature) ensemble. The ReaxFF force field was employed with parameters to describe interactions between Si/O/C/H atoms.^{34,35} Performing ReaxFF simulations rather than quantum mechanics calculations enabled us to investigate the dynamics of the system at a more extensive physical length scale and a longer timescale. Although the ReaxFF can provide a reasonable approximation of reactivity, it should be noted that the force field requires substantial validation for a specific system. MD simulations were performed using the Large Atomic/Molecular Massively Parallel Simulation (LAMMPS) software³⁶ and the post-

processing was carried out using OVITO software.³⁷ Additional details are provided in the Supplement Information.

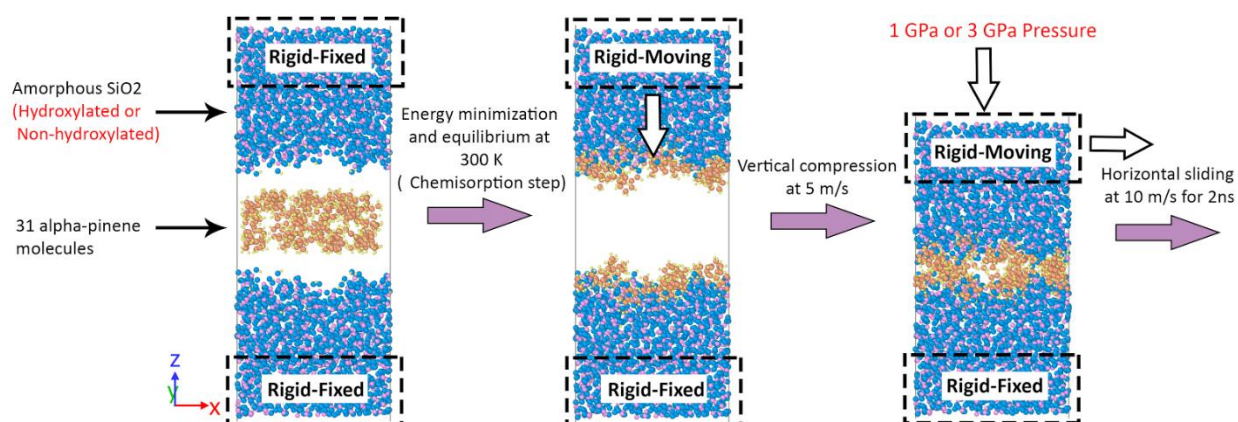


Figure 1. The configuration of the model system illustrating the three stages of the MD simulations. From left to right: energy minimization, compression, and sliding.

RESULTS AND DISCUSSION

Figure 2a shows the friction coefficients measured during VPL for the fully hydroxylated and thermally dehydroxylated silica surfaces. Thermal dehydroxylation was used as a means of making the surface more reactive. Another approach would be to pre-condition the surface under poor lubrication conditions [see Figure S1 in Supporting Information].³⁸ Surface wear under poor lubrication conditions would expose dangling bonds that can readily react with adsorbed molecules. Thermal dehydroxylation will occur through dehydrations reaction among adjacent hydroxyl groups forming siloxane bridges.³⁸ Such siloxane bonds at the surface would be subject to high strain (due to unfavorable bond angles) and thus have high reactivity.

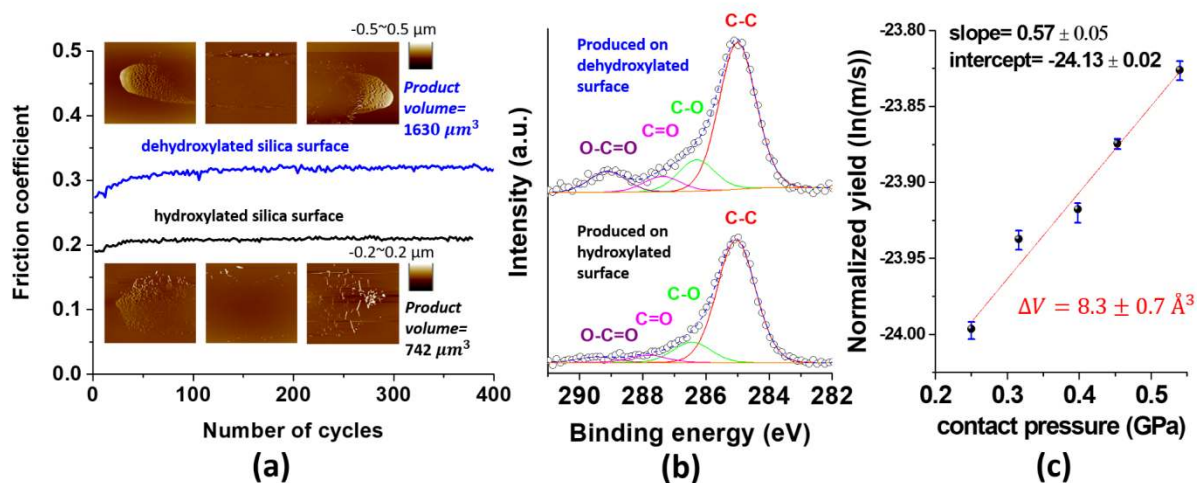


Figure 2. (a) Friction coefficients of hydroxylated and dehydroxylated surfaces in α -pinene VPL conditions at a 40 % partial pressure relative to saturation. A borosilicate ball was used as a counter-surface. The applied Hertzian contact pressure was 0.32 GPa and the sliding speed was 4 mm/s. Insets are AFM images of reaction products piled in and along the slide tracks. (b) C1s XPS spectra of the shear-induced polymers produced on silicon oxide surfaces with two different surface conditions. (c) Semi-log plot of the normalized tribo-polymer yield against the contact pressure for α -pinene sheared on the dehydroxylated silicon oxide surface.

For chemical analysis purposes, we used the thermally dehydroxylated surface because it allowed better control of the surface chemistry. The dehydroxylated surface became partially hydrophobic [see Figure S2]. Atomic force microscopy (AFM) imaging after the VPL tests provided accumulations of reaction products in and along the slide track (insets in Figure 2a). The dehydroxylated surface had a higher friction coefficient and significantly more products than the hydroxylated surface. The higher friction coefficient (~ 0.3) is within the typical range for polymer surfaces.³⁹ The C1s XPS analysis of the reaction products (Figure 2b) shows the presence of oxygen groups (C-O at ~ 286.5 eV, C=O at ~ 287.5 eV, and O-C=O at ~ 289 eV), even though α -pinene has no oxygen. The dehydroxylated surface produced more oxygenated products than the hydroxylated surface. These results imply that the surface chemistry of the solid substrate plays a critical role in reaction yield and pathways.

For the dehydroxylated surface, the shear-induced polymerization yield was high enough to conduct contact pressure dependence measurements to determine the critical activation volume (ΔV^*), as shown in Figure 2c.²⁹ This could not be done reliably on the hydroxylated surface because the reaction yield was too low to be measured with enough precision. Using an Arrhenius-type activated reaction model,^{11, 23, 40} the ΔV^* of this reaction was found to be about $8.3 \pm 0.7 \text{ \AA}^3$ on the dehydroxylated surface [see Supporting Information for calculation details]. This value corresponds to $\sim 3\%$ of the molecular volume of α -pinene in the liquid state (liquid molar volume divided by the Avogadro's number). In equilibrium conditions, molecules are incompressible. This then raises a question about the physical meaning of the volume change between the reactant and transition states of the molecule.

The molecular origins of the higher yield of shear-induced polymerization on the dehydroxylated surface, the production of oxygenated products from oxygen-free precursor molecules on silicon oxide, and the critical activation volume calculated from the pressure-dependence data could not be understood from the experimental studies alone; so, ReaxFF-MD simulations were performed to address these questions [see Figure 1]. Figures 3a and 3b show the molecular weight (MW) distribution of molecular species remaining after applying 1 GPa pressure for 2 ns without any lateral shear action. On both non-hydroxylated and hydroxylated surfaces, no association products of α -pinene molecules were observed. The slight increase in the molecular weights is due to the uptake of oxygen atoms from the silicon oxide substrates.

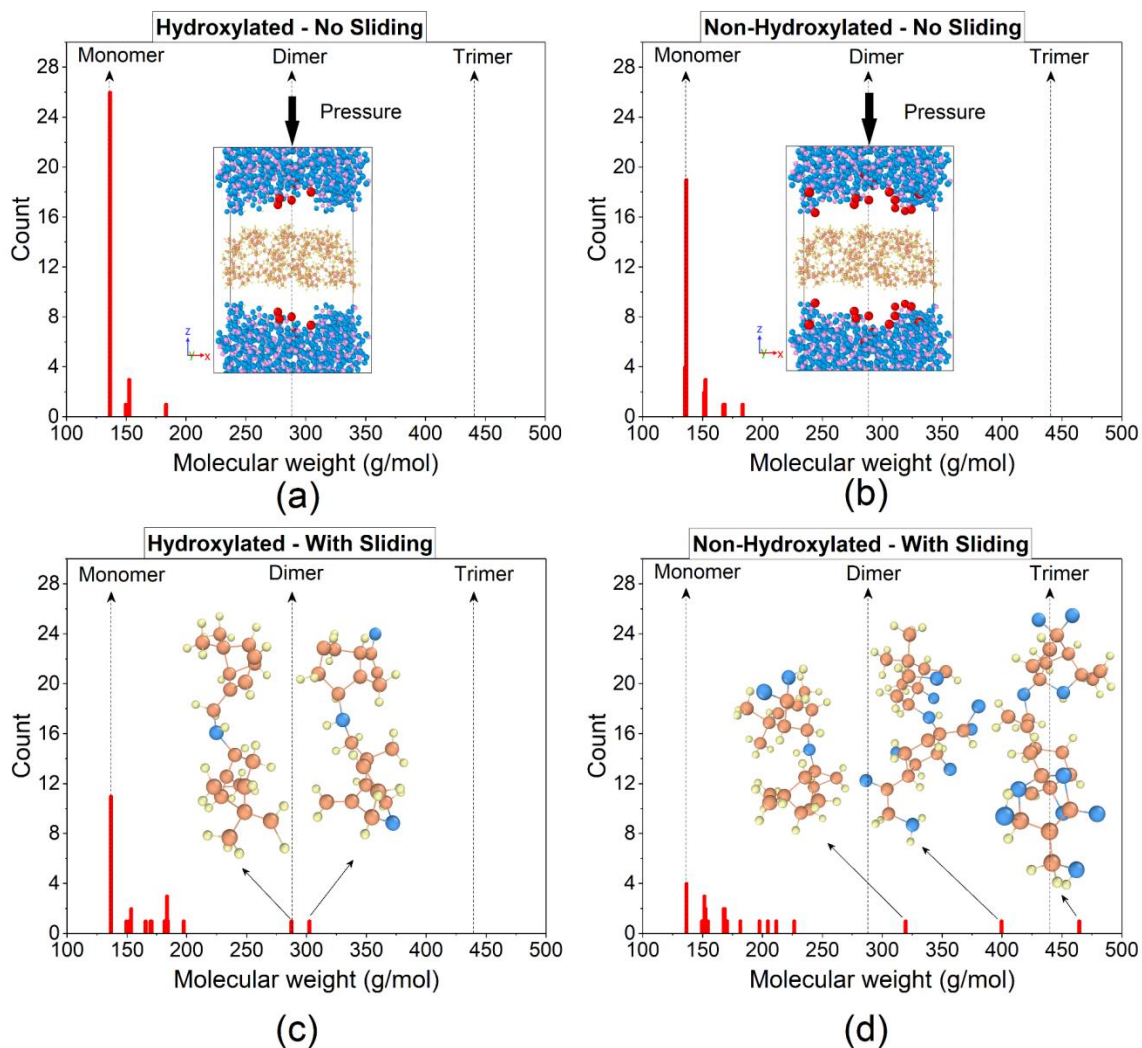


Figure 3. Histograms of the molecular weights of species with ten or more carbon atoms from simulations at 1 GPa for (a) hydroxylated surface without sliding, (b) non-hydroxylated surface without sliding, (c) hydroxylated surface after 2ns of sliding, and (d) non-hydroxylated surface after 2ns of sliding. Side view images of the MD simulations are shown as insets in (a) and (b), where reactive surface sites are highlighted by red spheres. Snapshots of representative shear-induced reaction products are shown as insets to (c) and (d).

Figures 3c and 3d show the MW distribution of species with 10 or more carbon atoms after shear. Here, the formation of shear-induced reaction products is evidenced by the presence of products whose MWs are heavier than dimers. The comparison with the control case without shear (Figures 3a and 3b) clearly shows that oligomerization does not occur without interfacial

shear; in other words, chemical reactions are facilitated or initiated by interfacial shear. There is significantly more oligomerization on the non-hydroxylated surface, which is congruent with the experimental result (Figure 2). Note that, due to the limited sliding time and number of reactant molecules in MD simulations, high MW products could not be formed.

In MD simulations, it was found that the increase in applied contact pressure from 1 GPa to 3 GPa resulted in more products at the end of sliding [see Figure S6a]. When these two data points were used for the Arrhenius-type activation model analysis, ΔV^* was estimated to be $\sim 6 \text{ \AA}^3$ on the non-hydroxylated surface [see Figure S6b]. Although accuracy of this value is limited due to insufficient data points, it is still intriguing to note that the simulation value is reasonably close to the experimentally determined ΔV^* (Figure 2c). These observed consistencies imply that the molecular details available in the ReaxFF-MD simulations are relevant to the experimental observations, despite the differences in size and time scales between the experimental and simulation conditions.

Figure 4 displays snapshots from the simulation following the trajectory of one α -pinene molecule. At $t = 114$ ps after initiation of sliding (Figure 4b), the surface O1 atom is approaching the C6 atom of the α -pinene molecule. At $t = 120$ ps (Figure 4c), the O1 atom is covalently bonded to the C6 atom; at $t = 124$ ps (Figure 4d), the second oxygen is attached to the C1 atom and the covalent bond between C1 and C6 is broken. Following the trajectories of all molecules forming association products, it was found that α -pinene molecules are first oxidatively activated by reactions with dangling oxygen groups at the surface before the sliding [see Figure S7] and/or hydroxyl groups during the sliding before they are associated with another molecule. This result indicates that the oxidative chemisorption or activation of the interfacial molecule is necessary for shear-induced oligomerization reactions to occur.

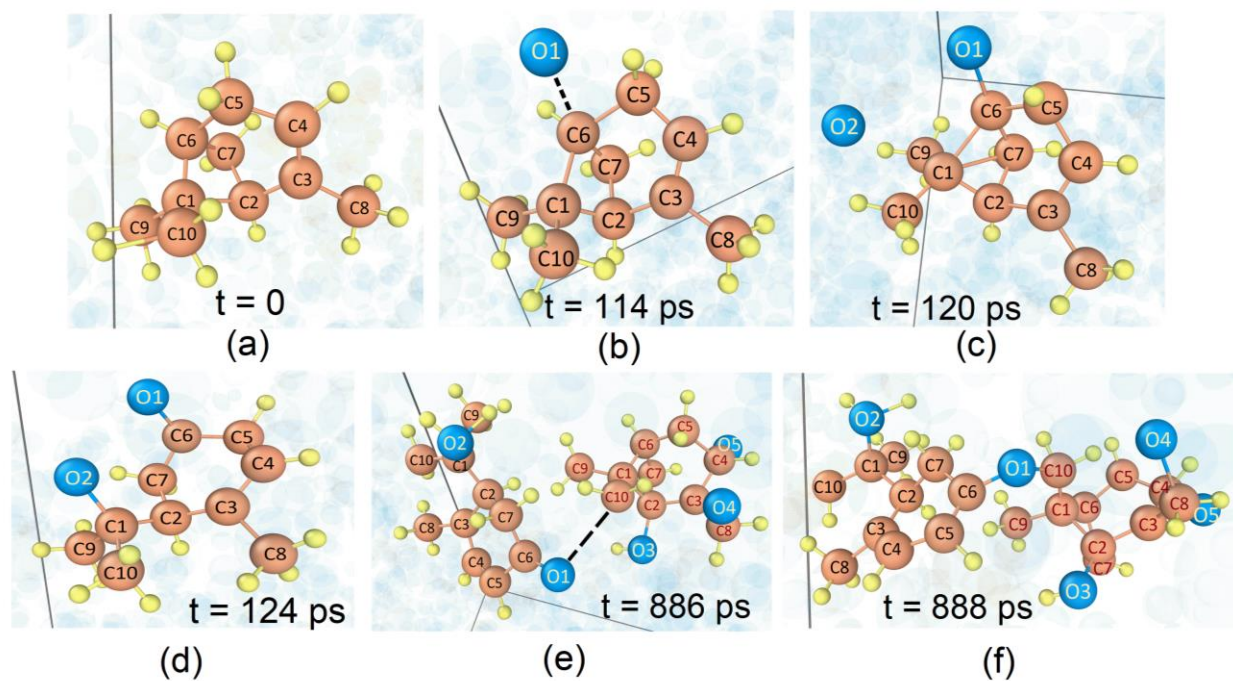


Figure 4. Snapshots at various times from ReaxFF-MD simulations following one α -pinene molecule. The numbers on atoms are given following the IUPAC nomenclature. The 4-membered ring consists of C1, C2, C7, and C6. The 6-membered ring is made of C2, C3, C4, C5, C6, and C7. The C=C double bond exists between C3 and C4. The C8, C9, and C10 are methyl side groups. The oxygen atoms are from the silicon oxide substrate and numbered following the order of covalent bond formation to α -pinene molecules. Atom colors correspond to: C-brown, O-blue, and H-yellow.

The oxidized intermediate species in Figure 4c meets with another α -pinene molecule at $t = 886$ ps (Figure 4e). Here, it is important to note that a covalent bond is formed between the O1 atom attached to the C6 of the first molecule and the C10 atom of the second molecule. For all 10 association products formed within the 2 ns simulation duration, the covalent bonds associating two molecules are formed between oxygen atoms of the oxidized intermediate species and the carbon atoms of the neighboring molecule [see Figure S8]. This is drastically different from typical catalytic polymerization reactions of α -pinene under thermal conditions, where cationic intermediates are formed and the polymerization proceeds through C-C covalent bond formation.⁴¹ This difference implies that thermal reaction mechanisms cannot be applied or utilized to explain mechanochemical reactions.

When the 10 oligomers produced in MD simulations are analyzed [Figure S8], it is found that the C=C double bonds in the 6-membered ring are more likely to be attacked by the oxygen atom of the intermediate species and activated by oxidation reactions with the surface. The next most likely association reaction appears to be with the 4-membered ring or methyl groups attached to the 4-membered ring. These are the highly strained regions within the α -pinene molecule. Although the number of products is not large enough to give reliable statistics, this trend suggests that the internal strain of molecules plays a critical role in mechanochemical reactions.

The role of internal strain in the oxidative activation of α -pinene forming intermediate species is shown in Figure 5. At $t = 98$ ps, the C1-C6 bond length (d_{C1-C6}) is slightly elongated from 1.5 Å to 1.75 Å, which is accompanied by an increase in the C2-C7-C6 bond angle (θ_7) and a decrease in θ_1 . This deformation appears to facilitate the association of C6 with O1 at $t = 106$ ps, at which time d_{O1-C6} decreases from 2.3 Å to 1.9 Å (still too far to covalently bond). Compared to the total energy for a small cluster of reacting species only, the physical deformation is found to substantially reduce the activation energy for the oxygen transfer from the surface to α -pinene [see Figures S9 and S10]. As O1 approaches C6 ($t = 106$ ps), d_{C1-C6} is elongated further to 1.9 Å, θ_6 decreases to 84°, and θ_7 increases further to 110°. This corresponds to Figure 4b. Finally, at $t = 124$ ps (which corresponds to Figure 4d), the covalent bond between O1 and C6 is formed (decreasing d_{O1-C6} to 1.5 Å). At the same time, O2 is covalently bonded to C1 (d_{O2-C1} decreases from ~3 Å to 1.5 Å); this is accompanied with the ring opening, which is evidenced by the increase of d_{C1-C6} from 1.9 Å to 3.4 Å and the increase of θ_2 and θ_7 to ~140°. Also, d_{C1-C2} , d_{C2-C7} , and d_{C6-C7} get slightly shorter by 0.1 Å (data not shown). During this entire process of forming the oxidized intermediate species, the effective volume change is about 10 Å³. In the subsequent association between the activated intermediate and α -pinene, the shear-induced deformation of the molecule is found to facilitate the C-O-C bond formation [see Figures S11 and S12].

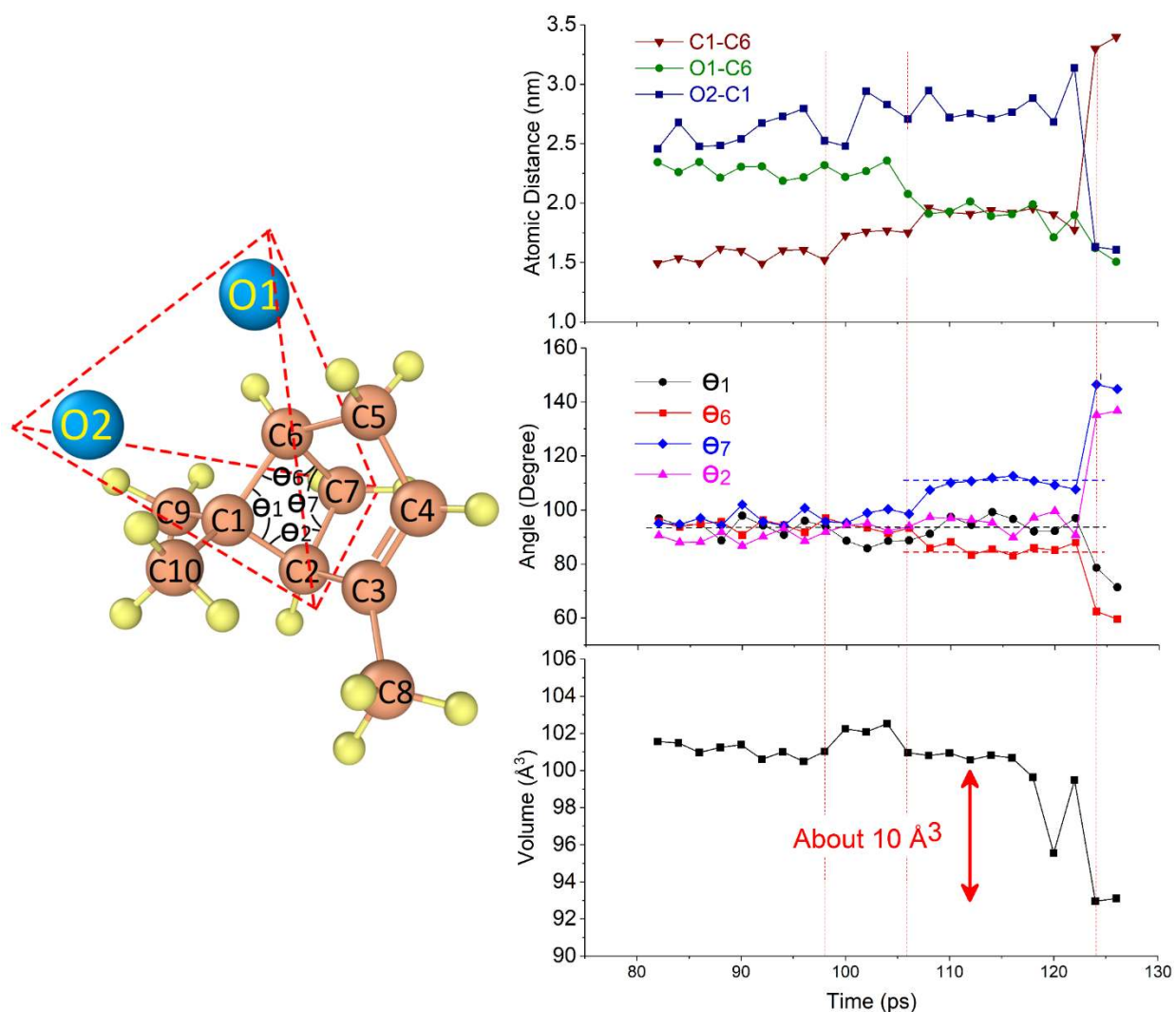


Figure 5. Physical deformation of the 4-membered ring during the oxidation of α -pinene by reaction with surface oxygen atoms (steps shown in Figures 4b, 4c, and 4d). Here, θ_1 , θ_2 , θ_7 , and θ_6 represent the C6-C1-C2, C1-C2-C7, C2-C7-C6, and C7-C7-C1 bond angles, respectively. The volume of a tetrahedral box (identified by dotted lines) is also shown.

MD simulation results also explain the XPS analysis data (Figure 2b) which indicate that the shear-induced polymerization products are highly oxidized. The polymerization occurs not through the formation of direct C-C covalent bond between two molecules, but through the formation of the C-O-C ether bond (responsible for the 286.5 eV peak in Figure 2b). Also, unreacted terminal oxygen atoms will be further oxidized, forming carbonyl or carboxyl groups

(287.5 eV, and 289 eV in Figure 2b) upon exposure to air. In simulations, the non-hydroxylated surface produces more oxidized products than the hydroxylated surface [see Figure S13], which is congruent with the XPS result showing more oxidized C1s components for the reaction products on the dehydroxylated surface (Figure 2b).

CONCLUSIONS

Vapor phase lubrication experiments of α -pinene sheared between hydroxylated and dehydroxylated silica surfaces provided an ideal test bed for exploring the effects of surface reactivity on mechanically driven chemical reactions. Measurements of friction during sliding and characterization of the resultant reaction products revealed higher yield on the dehydroxylated surface, the formation of oxygenated products from oxygen-free precursor molecules, and an activation volume corresponding to $\sim 3\%$ of the molar volume of α -pinene. Reactive MD simulations of hydroxylated and non-hydroxylated surfaces provided atom-scale explanations for these observations. First, non-hydroxylated surfaces were shown to react more with the α -pinene and have more oligomerization during shear than the hydroxylated surfaces. Also, the activation volumes calculated from the pressure-dependence of the yield in experiments and simulations for the non-hydroxylated surface were comparable to each other. This consistency with experimental observations indicated the simulations were indeed relevant to the experiments and supported the hypothesis that more reactivity of the substrate surface corresponds to higher oligomerization yield during shear. Second, the simulations showed that oligomerization between two α -pinene molecules occurs via oxygen atoms obtained from surface reactions, providing direct evidence of the connection between surface reactivity and yield. Lastly, detailed analysis of individual molecules during the simulation revealed that shear facilitates association reactions through deformation of strained parts of the molecule, which in turn enables the molecule to bond with surface oxygen as the first step towards oligomerization.

SUPPORTING INFORMATION: Activation of the silica substrate surface by rubbing in poorly lubricated condition in experiment; Water contact angle on fully hydroxylated and thermally dehydroxylated silica surfaces; Creation of amorphous SiO₂ model structure; Hydroxylation of the model SiO₂ surface; Pressure dependence of the oligomerization and critical activation volume calculation; Surface dependence of chemisorption before sliding;

Association of two molecules via C-O-C bond formation; Comparison of total energy changes for selected reaction paths; Distribution of oxygen atoms in the shear-induced association reaction products.

ACKNOWLEDGEMENTS. This work was carried out with the support from the National Science Foundation (Grant No. CMMI-1435766, 1727571, 1727356).

AUTHOR CONTRIBUTIONS

The entire scope of this work was designed by SHK and AM. AK carried out the ReaxFF simulations, JY performed the energy barrier calculations, and XH conducted experimental work. SHK, AM, AK and XH contributed to the manuscript writing.

REFERENCES

1. Spikes, H., Stress-augmented thermal activation: Tribology feels the force. *Friction* **2018**, *6* (1), 1-31.
2. Do, J.-L.; Friščić, T., Mechanochemistry: A Force of Synthesis. *ACS central science* **2016**, *3* (1), 13-19.
3. Makarov, D. E., Perspective: Mechanochemistry of biological and synthetic molecules. *The Journal of chemical physics* **2016**, *144* (3), 030901.
4. Li, Y.-S.; Shyy, J.; Li, S.; Lee, J.; Su, B.; Karin, M.; Chien, S., The Ras-JNK pathway is involved in shear-induced gene expression. *Molecular and Cellular Biology* **1996**, *16* (11), 5947-5954.
5. Wang, H.; Riha, G. M.; Yan, S.; Li, M.; Chai, H.; Yang, H.; Yao, Q.; Chen, C., Shear stress induces endothelial differentiation from a murine embryonic mesenchymal progenitor cell line. *Arteriosclerosis, thrombosis, and vascular biology* **2005**, *25* (9), 1817-1823.
6. Sriram, K.; Laughlin, J. G.; Rangamani, P.; Tartakovsky, D. M., Shear-induced nitric oxide production by endothelial cells. *Biophysical journal* **2016**, *111* (1), 208-221.
7. Beyer, M. K.; Clausen-Schaumann, H., Mechanochemistry: the mechanical activation of covalent bonds. *Chemical Reviews* **2005**, *105* (8), 2921-2948.
8. Chen, Z.; Mercer, J. A.; Zhu, X.; Romaniuk, J. A.; Pfattner, R.; Cegelski, L.; Martinez, T. J.; Burns, N. Z.; Xia, Y., Mechanochemical unzipping of insulating poly(ladderene) to semiconducting polyacetylene. *Science* **2017**, *357* (6350), 475-479.
9. Felts, J. R.; Oyer, A. J.; Hernández, S. C.; Whitener Jr, K. E.; Robinson, J. T.; Walton, S. G.; Sheehan, P. E., Direct mechanochemical cleavage of functional groups from graphene. *Nature communications* **2015**, *6*, 6467.

10. Bhaskaran, H.; Gotsmann, B.; Sebastian, A.; Drechsler, U.; Lantz, M. A.; Despont, M.; Jaroenapibal, P.; Carpick, R. W.; Chen, Y.; Sridharan, K., Ultralow nanoscale wear through atom-by-atom attrition in silicon-containing diamond-like carbon. *Nature nanotechnology* **2010**, *5* (3), 181-185.
11. Jacobs, T. D.; Carpick, R. W., Nanoscale wear as a stress-assisted chemical reaction. *Nature nanotechnology* **2013**, *8* (2), 108-112.
12. Zhang, J.; Spikes, H., On the mechanism of ZDDP antiwear film formation. *Tribology Letters* **2016**, *63* (2), 1-15.
13. Alazizi, A.; Barthel, A. J.; Surdyka, N. D.; Luo, J.; Kim, S. H., Vapors in the ambient—A complication in tribological studies or an engineering solution of tribological problems? *Friction* **2015**, *3* (2), 85-114.
14. He, H.; Qian, L.; Pantano, C. G.; Kim, S. H., Mechanochemical Wear of Soda Lime Silica Glass in Humid Environments. *Journal of the American Ceramic Society* **2014**, *97* (7), 2061-2068.
15. Ito, K.; Martin, J. M.; Minfray, C.; Kato, K., Formation Mechanism of a Low Friction ZDDP Tribofilm on Iron Oxide. *Tribology Transactions* **2007**, *50* (2), 211-216.
16. James, S. L.; Adams, C. J.; Bolm, C.; Braga, D.; Collier, P.; Friscic, T.; Grepioni, F.; Harris, K. D. M.; Hyett, G.; Jones, W.; Krebs, A.; Mack, J.; Maini, L.; Orpen, A. G.; Parkin, I. P.; Shearouse, W. C.; Steed, J. W.; Waddell, D. C., Mechanochemistry: opportunities for new and cleaner synthesis. *Chemical Society Reviews* **2012**, *41* (1), 413-447.
17. Eyring, H., Viscosity, plasticity, and diffusion as examples of absolute reaction rates. *The Journal of chemical physics* **1936**, *4* (4), 283-291.
18. Zhurkov, S. N. In *Kinetic concept of the strength of solids*, ICF1, Japan 1965, 1965.
19. Prandtl, L., Ein Gedankenmodell zur kinetischen Theorie der festen Körper. *ZAMM-Journal of Applied Mathematics and Mechanics/Zeitschrift für Angewandte Mathematik und Mechanik* **1928**, *8* (2), 85-106.
20. Drummond, C.; Israelachvili, J.; Richetti, P., Friction between two weakly adhering boundary lubricated surfaces in water. *Physical Review E* **2003**, *67* (6), 066110.
21. Briscoe, B.; Evans, D. In *The shear properties of Langmuir-Blodgett layers*, Proceedings of the Royal Society of London A: Mathematical, Physical and Engineering Sciences, The Royal Society: 1982; pp 389-407.
22. Kauzmann, W.; Eyring, H., The viscous flow of large molecules. *Journal of the American Chemical Society* **1940**, *62* (11), 3113-3125.
23. Spikes, H.; Tysoe, W., On the Commonality Between Theoretical Models for Fluid and Solid Friction, Wear and Tribochemistry. *Tribology Letters* **2015**, *59* (1), 21.

24. Murphy, K. L.; Tysoe, W. T.; Bennett, D. W., A comparative investigation of aryl isocyanides chemisorbed to palladium and gold: An ATR-IR spectroscopic study. *Langmuir* **2004**, *20* (5), 1732-1738.
25. Murphy, K.; Azad, S.; Bennett, D.; Tysoe, W., Adsorption, decomposition and isomerization of methyl isocyanide and acetonitrile on Pd (111). *Surface science* **2000**, *467* (1), 1-9.
26. Yeon, J.; He, X.; Martini, A.; Kim, S. H., Mechanochemistry at Solid Surfaces: Polymerization of Adsorbed Molecules by Mechanical Shear at Tribological Interfaces. *ACS Applied Materials & Interfaces* **2017**, *9* (3), 3142-3148.
27. He, X.; Kim, S. H., Surface Chemistry Dependence of Mechanochemical Reaction of Adsorbed Molecules□ An Experimental Study on Tribopolymerization of α -Pinene on Metal, Metal Oxide, and Carbon Surfaces. *Langmuir* **2018**, *34* (7), 2432-2440.
28. Barthel, A. J.; Al-Azizi, A.; Surdyka, N. D.; Kim, S. H., Effects of gas or vapor adsorption on adhesion, friction, and wear of solid interfaces. *Langmuir* **2013**, *30* (11), 2977-2992.
29. He, X.; Kim, S. H., Mechanochemistry of Physisorbed Molecules at Tribological Interfaces: Molecular Structure Dependence of Tribochemical Polymerization. *Langmuir* **2017**, *33* (11), 2717-2724.
30. Hickenboth, C. R.; Moore, J. S.; White, S. R.; Sottos, N. R.; Baudry, J.; Wilson, S. R., Biasing reaction pathways with mechanical force. *Nature* **2007**, *446* (7134), 423-427.
31. Kean, Z. S.; Niu, Z.; Hewage, G. B.; Rheingold, A. L.; Craig, S. L., Stress-responsive polymers containing cyclobutane core mechanophores: reactivity and mechanistic insights. *Journal of the American Chemical Society* **2013**, *135* (36), 13598-13604.
32. He, X.; Barthel, A. J.; Kim, S. H., Tribochemical synthesis of nano-lubricant films from adsorbed molecules at sliding solid interface: Tribo-polymers from α -pinene, pinane, and n-decane. *Surface Science* **2016**, *648*, 352-359.
33. Barthel, A. J.; Kim, S. H., Lubrication by physisorbed molecules in equilibrium with vapor at ambient condition: effects of molecular structure and substrate chemistry. *Langmuir* **2014**, *30* (22), 6469-6478.
34. Senftle, T. P.; Hong, S.; Islam, M. M.; Kylasa, S. B.; Zheng, Y.; Shin, Y. K.; Junkermeier, C.; Engel-Herbert, R.; Janik, M. J.; Aktulga, H. M., The ReaxFF reactive force-field: development, applications and future directions. *npj Computational Materials* **2016**, *2*, 15011.
35. Van Duin, A. C.; Dasgupta, S.; Lorant, F.; Goddard, W. A., ReaxFF: a reactive force field for hydrocarbons. *The Journal of Physical Chemistry A* **2001**, *105* (41), 9396-9409.
36. Plimpton, S., Fast parallel algorithms for short-range molecular dynamics. *Journal of computational physics* **1995**, *117* (1), 1-19.
37. Stukowski, A., Visualization and analysis of atomistic simulation data with OVITO—the Open Visualization Tool. *Modelling and Simulation in Materials Science and Engineering* **2009**, *18* (1), 015012.

38. Banerjee, J.; Bojan, V.; Pantano, C. G.; Kim, S. H., Effect of heat treatment on the surface chemical structure of glass: Oxygen speciation from in situ XPS analysis. *Journal of the American Ceramic Society* **2018**, *101* (2), 644-656.
39. Santner, E.; Czichos, H., Tribology of polymers. *Tribology International* **1989**, *22* (2), 103-109.
40. Gosvami, N.; Bares, J.; Mangolini, F.; Konicek, A.; Yablon, D.; Carpick, R., Mechanisms of antiwear tribofilm growth revealed in situ by single-asperity sliding contacts. *Science* **2015**, *348* (6230), 102-106.
41. Binet, M. L.; Commereuc, S.; Verney, V., Thermo-oxidation of polyterpenes: influence of the physical state. *European Polymer Journal* **2000**, *36* (10), 2133-2142.

TOC Graphic

